Interactive comment on“Centennial-scale monsoon changes since the last deglaciation linked to solar activities and North Atlantic cooling” by Xingxing Liu et al.

Anonymous Referee #1

Received and published: 25 October 2019

The manuscript entitled "Centennial-scale monsoon changes since the last deglaciation linked to solar activities and North Atlantic cooling" illustrates the change of EASM and EAWM in western Chinese Loess Plateau and its centennial determinants, namely solar activity and AMOC over an extended period. The value of this study is to provide a relatively high-resolution paleo-climatic record in western Chinese Loess Plateau spanned 16000 years. Given the originality of this paleo-climate record, I will recommend this paper to be accepted for publication. However, there are a couple of issues should be addressed prior to the acceptance of this manuscript. My comments are detailed below:

1. In your early article (liu et al., 2015, Aeolian Research), From 6 to 13 m, this same section included two fluvio-aeolian layers at 7.2-7.5m and 10.1-10.6m. Moreover, these fluvio-aeolian layers are identified by relatively fine mean grain-size and low magnetic susceptibility during the BA and early Holocene period, according to your age model. Moreover, paleoflood events were found in middle and upper Yellow River basin during the early Holocene and BA period (Guo et al., 2017, Journal of Hydrology; li et al., 2014,QR),

Reply: We agree with the reviewer’s point that these fluvio-aeolian layers at 7.2-7.5m and 10.1-10.6m are flood slackwater deposits (SWD) (Baker et al., 1983; Huang et al., 2012, 2013; Li et al., 2014; Guo et al., 2017). The SWDs are typified by their relatively fine mean grain-size and low magnetic susceptibility, which are often preserved in backwater areas after flood recession (Huang et al., 2012, 2013; Vandenberghe et al., 2018).

2. As you mention whether Titanium in Huguang Maar Lake is a proxy for local hydrology or EAWM intensity, this record is very controversial. So, in Figure 3, I suggest you find a more reliable EAWM record to compare with your EAWM record. Moreover, I find, on the long-term

interval during the Holocene, your EASM record isn't also consistent with the SMI record from Qinghai lake and $\delta^{18}O$ record from Dongge Cave, I suggest you find other high-resolution EASM records to compare with your data, though you mention they share similar centennial-scale climate changes.

Reply: Thanks for this comment. Although whether Titanium (Ti) in Huguang Maar Lake is a proxy for local hydrology or EAWM intensity remains controversial, it's the only one high resolution EAWM record we can compare with so far. Similarly, when we discuss about centennial to millennial-scale monsoon events, we have to choose some high resolution EASM records. Here we added the record of precipitation reconstruction from Lake Gonghai (Chen et al., 2015; Liu et al., 2015, 2017) in Fig. 3 and related discussions about the long-term trend of EASM since the last deglaciation.

3. In your manuscript, you mainly discuss centennial-scale monsoon changes. But I find, after you removed the long-term trend, these remaining sequences obviously show 1 ka and 1.27 ka cycle. I suggest they represent the millennial-scale climate changes rather than the centennial-scale changes.

Reply: Thanks for this comment. We change the title into "Centennial to millennial-scale monsoon changes since the last deglaciation linked to solar activities and North Atlantic cooling".

References

Baker, V.R., Kochel, R.C., Patton, P.C., and Pickup, G.: Palaeohydrologic analysis of Holocene flood slack-water sediments. Modern and ancient fluvial systems, 229-239, 1983.

Chen, F., Xu, Q., Chen, J., Birks, H.J.B., Liu, J., Zhang, S., Jin, L., An, C., Telford, R.J., Cao, X., Wang, Z., Zhang, X., Selvaraj, K., Lu, H., Li, Y., Zheng, Z., Wang, H., Zhou, A., Dong, G., Zhang, J., Huang, X., Bloemendal, J., and Rao, Z.: East Asian summer monsoon precipitation variability since the last deglaciation, Scientific Reports, 5, 11186, 2015.

Guo, Y.Q., Huang, C.C., Pang, J.L., Zhou, Y.L., Zha, X.C., and Miao, P.N.: Reconstruction palaeoflood hydrology using slackwater flow depth method in the Yanhe River valley, middle Yellow River basin, China[J]. Journal of hydrology, 544: 156-171, 2017.

Huang, C.C., Pang, J.L., Zha, X.C., Zhou, Y.L., Yin, S.Y., Su, H.X., Zhou, L., and Yang, J.C.: Extraordinary hydro-climatic events during the period AD 200– 300 recorded by slackwater deposits in the upper Hanjiang River valley, China. Palaeogeography, Palaeoclimatology, Palaeoecology, 374: 274-283, 2013.

Huang, C.C., Pang, J.L., Zha, X.C., Zhou, Y.L., Su, H.X., Zhang,Y.Z., Wang, H.S., and Gu, H.L.:

Holocene palaeoflood events recorded by slackwater deposits along the lower Jinghe River valley, middle Yellow River basin, China. Journal of Quaternary Science, 27(5): 485-493, 2012.

Li, G.Q., Dong, G.H., Wen, L.J., and Chen, F.H.: Overbank flooding and human occupation of the Shalongka site in the Upper Yellow River Valley, northeast Tibet Plateau in relation to climate change since the last deglaciation. Quaternary research, 82(2): 354-365, 2014.

Liu, J.B., Chen, J.H., Zhang, X.J., Li, Y., Rao, Z.G., and Chen, F.H.: Holocene East Asian summer monsoon records in northern China and their inconsistency with Chinese stalagmite δ18O records. Earth-Science Reviews, 148: 194-208, 2015.

Liu, J.B., Rühland, K. M., Chen, J. H., Xu, Y. Y., Chen, S. Q., Chen, Q. M., Huang, W., Xu, Q. H., Chen, F. H., and Smol, J. P.: Aerosol-weakened summer monsoons decrease lake fertilization in the Chinese Loess Plateau. Nature Climate Change, 7, 190-194, 2017.

Vandenberghe, J., Sun, Y.B., Wang, X.Y., Abels, H.A., and Liu, X.X.: Grain-size characterization of reworked fine-grained aeolian deposits. Earth-science reviews, 177: 43-52, 2018.

Interactive comment on“Centennial-scale monsoon changes since the last deglaciation linked to solar activities and North Atlantic cooling” by Xingxing Liu et al.

Anonymous Referee #2

Received and published: 8 November 2019

Comment on Liu et al. CP_2019_119 Title: Centennial-scale monsoon changes since the last deglaciation linked to solar activities and North Atlantic cooling Authors: Xingxing Liu, Youbin Sun, Jef Vandenberghe, Peng Cheng, Xu Zhang, Evan J Gowan, Gerrit Lohmann, Zhisheng An

In this study, a 13.5 m-long terrace succession (DDW) was retrieved from Dadiwan, on the western margin of Chinese Loess Plateau (CLP), to investigate the variation of rapid monsoon changes since the last deglaciation. The entire sequence was dated with 12 radiocarbon ages. In this study, the authors proposed that Zr/Rb and Rb/Sr ratios can be used as proxies for East Asian winter monsoon (EAWM) and East Asian summer monsoon (EASM), respectively. In addition, the authors found an anti-phase relationship between the EAWM and EASM on centennial timescale during 16-1 ka BP. Comparing with North Atlantic cooling and solar activity proxies, the authors found that both factors dominated the East Asian monsoon (EAM) system during the early Holocene. But during the late Holocene, solar activity was no longer the main controlling factor of EAM. In general, the new data in this study could deepen our understanding of paleo EAM variations since the last deglaciation and the manuscript is worth publishing in this journal. However, this manuscript still has following shortcomings:

General comments:

1. Line 154-158: The authors said that grain size and magnetic susceptibility have been widely used as proxies for EAWM and EASM, respectively. Based on the fact that Zr/Rb and Rb/Sr ratios are highly consistent with grain size and magnetic susceptibility in the same sequence, the authors deduced that Zr/Rb and Rb/Sr ratios also can represent EAWM and EASM. If so, why don’t you use grain size and magnetic susceptibility in this study? What are the advantages of Zr/Rb and Rb/Sr ratios ?

Reply: The split cores were scanned every 5-mm using an Avaatech XRF core scanner. After core scanning, sub-samples were taken at contiguous 1-cm intervals for grain size and magnetic susceptibility analyses. The higher resolution of XRF scanning will be better for us to obtain "Centennial to millennial-scale monsoon changes".

2. In this study, the authors suggested that coarser particles in the sequence can be used as an indicator of stronger EAWM. However, it should be noteworthy that the dryland expanded southward during weak EASM periods. In this condition, coarse particles also could be transported to the study site even under a weak EAWM condition. Previous study suggested the advance-retreat cycles of desert is a dominant factor of grain-size, rather than winter monsoon (Ding et al., 1999). How do you corroborate that your EAWM proxy is reliable ?

Ding, Z.L., Sun, J.M., Rutter, N.W., et al., 1999. Changes in sand content of loess deposits along a North – South transect of the Chinese Loess Plateau and the implications for desert variations. Quaternary Research, 52, 56-62.

Reply: Thanks for this comment. We agree with the reviewer's point that the advance-retreat cycles of desert can influence the grain size, especially on the sand content (>63 μm) of loess deposits (Ding et al., 1999). Due to gravity effect, sand particles can be transported only a limited distance. At the DDW section, the sand content varies between about 0% and 10.5% in paleosol units and between about 0% and 19.6% in loess (see below). Such low sand content in both paleosol and loess suggests that the location of the desert margin has a potential influence on the grain size of DDW section. Furthermore, the gradient of grain-size change on the Loess Plateau was not constant, which show stronger gradient in cold periods and weaker gradient in warm periods. This phenomenon can only be explained by different wind intensities during different climatic periods. In other words, if the variations in grain sizes would be determined by shifting deflation zones, these gradients should be constant in each climate, which is not the case (Nugteren and Vandenberghe, 2004).

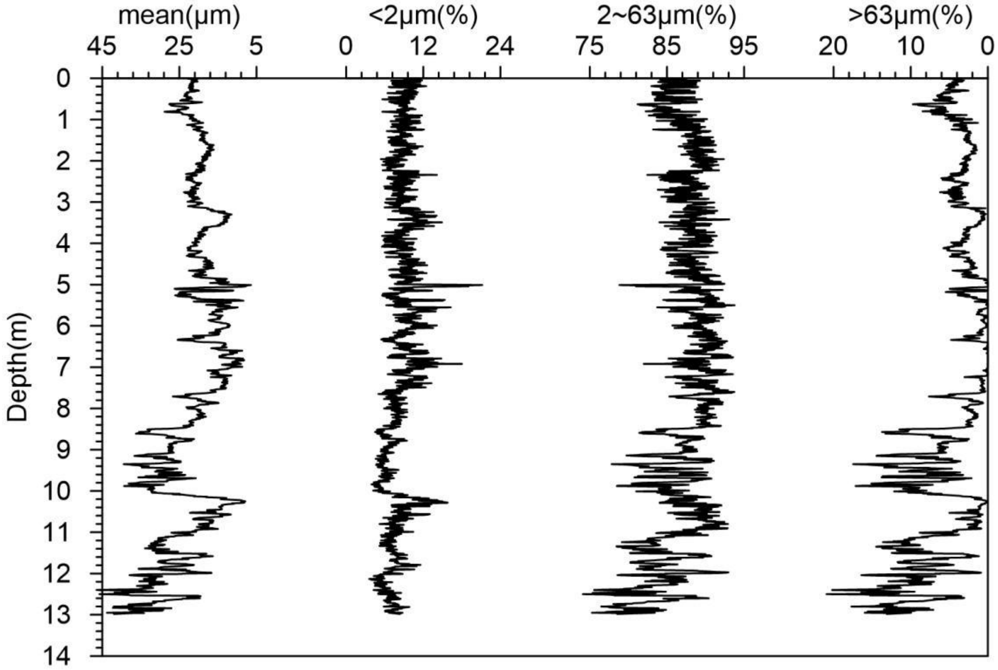

Fig. 1. Down-core variations of mean grain size and contents of three size fractions (＜2 μm, 2~63 μm and ＞63μm) of the DDW core

3. Line 180-192: I’m not convinced that EASM changes recorded by DDW are consistent with the Lake Qinghai summer monsoon index (SMI) and the $\delta^{18}O$ record from Dongge Cave stalagmites. First of all, records from Lake Qinghai and Dongge Cave show a large fluctuation form YD to early Holocene, but the variation of Rb/Sr ratio is smooth. Secondly, Rb/Sr ratio of DDW indicate that EASM during the middle and late Holocene is stronger than early Holocene, which is opposite with the records from Lake Qinghai and Dongge Cave. Thirdly, the highest Rb/Sr ratio occurred during the middle Holocene, indicating a mid-Holocene EASM maximum. But both Lake Qinghai and Dongge Cave records show an early-Holocene EASM maximum. In fact, the result of mid-Holocene EASM maximum is consistent with a well-dated, pollen-based precipitation reconstruction from Lake Gonghai (Chen et al., 2015). The pollen record from Lake Gonghai has a resolution of ~ 20 yr, which is sufficient to reveal centennial-scale summer monsoon changes. I recommend the authors to add this record for comparison in Fig. 3. By the way, although $\delta^{18}O$ records from stalagmites have attracted extensive attention in paleoclimate studies due to their precise age controls, the interpretation of speleothem $\delta^{18}O$ in China remains controversial (e.g., Liu et al., 2015). Especially in recent years, more and more evidences

indicated that that cave speleothem δ^{18}O records in China cannot be used as a reliable proxy of EASM rainfall. The authors should notice this issue when using stalagmite δ^{18}O record.

Chen, F.H., Xu, Q.H., Chen, J.H., et al., 2015. East Asian summer monsoon precipitation variability since the last deglaciation. Scientific Reports, 5, 11186.

Liu, J.B., Chen, J.H., Zhang, X.J., et al., 2015. Holocene East Asian summer monsoon records in northern China and their inconsistency with Chinese stalagmite δ 18O records. Earth Science Reviews, 148, 194-208.

Reply: Thanks for this comment. In the revision, we added the record of precipitation reconstruction from Lake Gonghai in Fig. 3 and related discussions (See below).

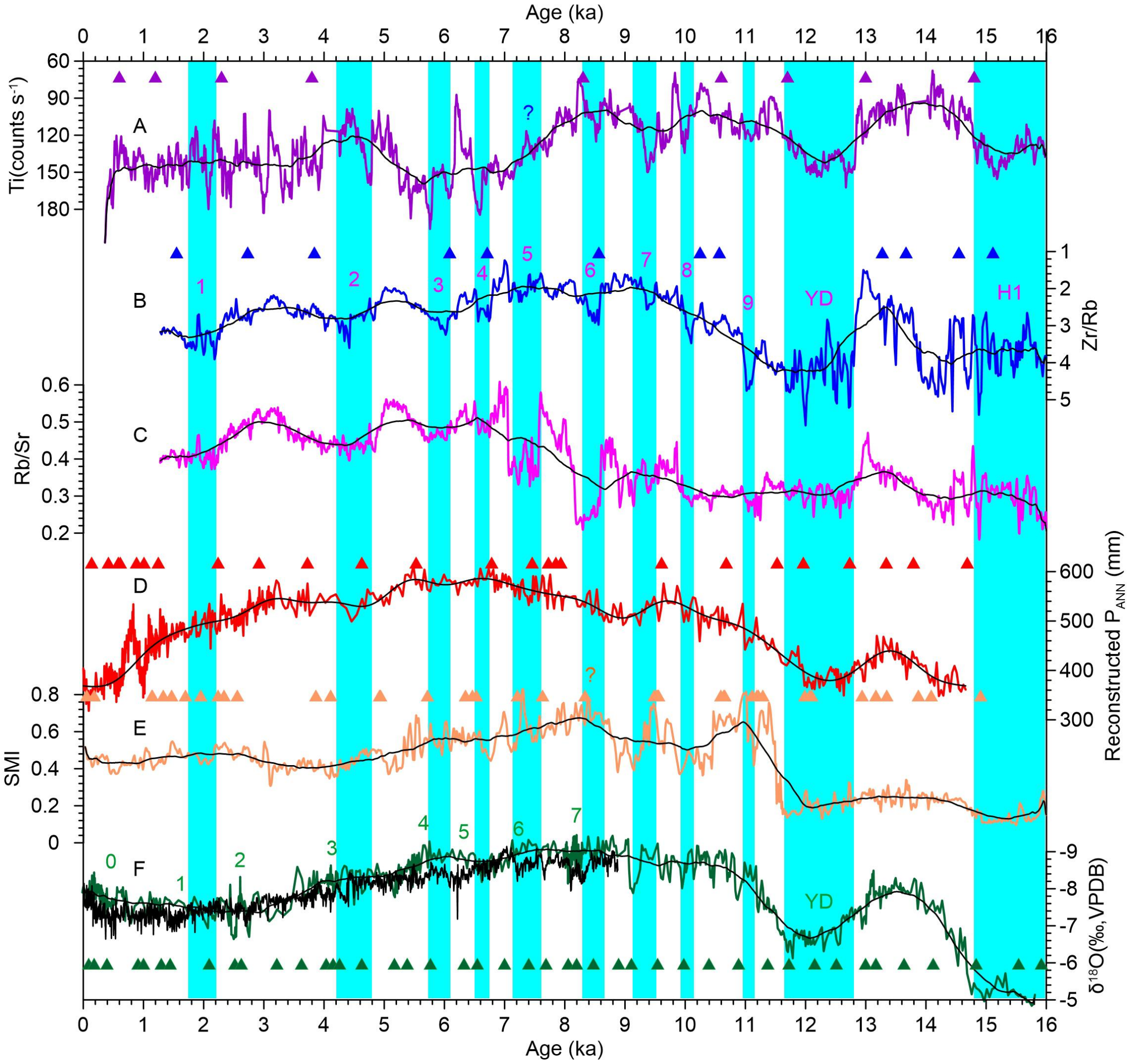

Fig 3. Comparisons of DDW records and other paleoclimatic records. (A) Ti content of Lake Huguang Maar (Yancheva et al., 2007); (B) Zr/Rb of DDW core; (C) Rb/Sr of DDW core; (D)

Pollen-based annual precipitation (PANN) reconstructed from Gonghai Lake (Chen et al., 2015); (E) Lake Qinghai summer monsoon index (SMI) (An et al., 2012); (F) Speleothem δ18O from Dongge Cave (Dykoski et al., 2005; Wang et al., 2005). AMS 14C ages are marked on the records of Lake Huguang Maar (Purple triangle), DDW (Blue triangle), Gonghai Lake (Red triangle), and Lake Qinghai (Peach triangle), respectively. The 230Th ages (Green triangle) are shown on the speleothem records. The cyan bars indicate the timing of abrupt monsoon events in different records.

Orbital trend of EASM intensity from DDW generally resembles the Pollen-based annual precipitation (PANN) reconstructed from Gonghai Lake (Fig.3D) (Chen et al., 2015; Liu et al., 2015, 2017), indicate a mid-Holocene climatic optimum (Liu et al., 2015). This suggests that EASM intensity not only follows changes in insolation inferred from the Lake Qinghai summer monsoon index (SMI) (Fig. 3E) (An et al., 2012) and stalagmite δ 18O records in eastern China (Fig. 3F) (Dykoski et al., 2005; Wang et al., 2005), but was also strongly moderated by the internal feedback processes such as continuous freshwater input into the North Atlantic caused by the remnant melting Laurentide ice sheet (Chen et al., 2015). In addition to this, asynchronous changes among these proxies can be possible due to varied sensitivity of these proxies and archives to changes in the monsoon intensity (Caley et al., 2014).

Compared with other summer monsoon proxy records in China, the centennial-scale EASM changes at DDW are consistent with the PANN reconstructed from Gonghai Lake (Fig.3D) (Chen et al., 2015; Liu et al., 2015, 2017) and SMI from Lake Qinghai (Fig. 3E) (An et al., 2012). Almost all the weak summer monsoon intervals, within dating errors, appear to coincide with major changes in the PANN reconstruction and SMI. It is worth noting that 8.2 ka event was not significant in the Gonghai (Fig. 3D) and Qinghai Lake (Fig. 3E). This could be ascribed to age model discrepancies, or the variable sensitivity of different proxies to changes in monsoon intensity (Chen et al., 2015). However, there are some discrepancies between Rb/Sr ratio of DDW and the and δ 18O record from Dongge Cave stalagmites in eastern China (Fig. 3F) (Dykoski et al., 2005; Wang et al., 2005). This discrepancy might attribute to the controversial paleoclimatic significance of δ 18O records from caves in southern China, or the North-South differences for the monsoon intensity (Caley et al., 2014; Tan, 2014; Liu et al., 2015; Chen et al., 2016).

Therefore, the weak EASM intervals existing in all these three different regions (CLP, northeast of Tibetan Plateau and eastern China) may have recorded centennial EASM variability since the last deglaciation.

4. The spectral results reveal that HSG, Zr/Rb and Rb/Sr records both display a prominent periodicity at 1.27 kyr during the late Holocene. Then the authors suggested that North Atlantic cooling were the major forcing of EAM system. However, in Figure 4, âUs14C, Zr/Rb and Rb/Sr also have a prominent periodicity at ~ 0.7 kyr, which indicated that solar activity could also contribute to EAM during the late Holocene. But it seems that periodicity of ~ 0.7 kyr is missed during explanation.

Reply: Thanks for this comment. Actually the second dominant periodicities (red line, see below) are not the same in the HSG, Zr/Rb and △^{14}C spectrum, and it's not evident in the Rb/Sr spectrum. This indicate that solar activities is not the direct cause of centennial summer monsoon variability. Compare to the ealry Holocene, there is a decrease of summer insolation and the small-amplitude fluctuations of solar activities during the late Holocene (Fig. 4D) (Berger, 1978). This is probably why it play a less important role in EAM system.

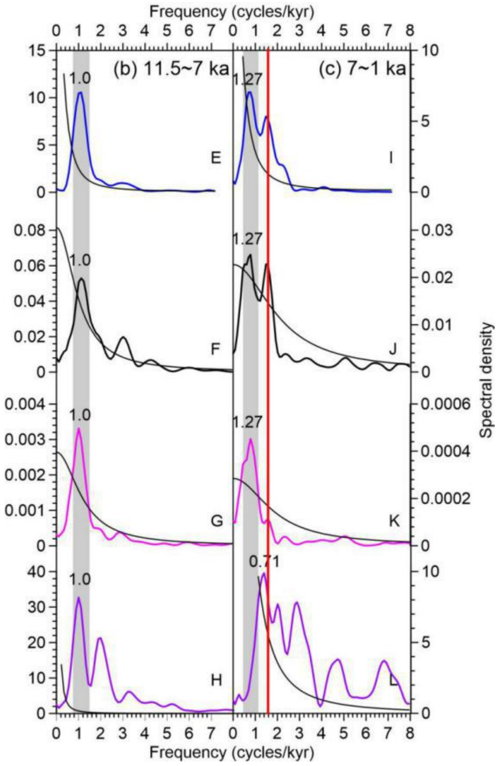

Fig. 4. The spectra results of the proxy records during the early (b) and late Holocene (c).

Specific comments:

1. Line 81-82: Source of climatic information of Qin'an Country is unclear. The authors should cite related references.

Reply: Meteorological data come from the national daily dataset of surface weather profile provided by the National Meteorological Data Center, http://data.cma.cn/data/.

2. Line 125: It would be better if the authors give the interpretation of "x" and "y" in the regression equation ($y=1.1465x+1.2546$).

Reply: x is the depth in m, y is the calculated age (cal ka BP)

3. I noticed that the 12 radiocarbon ages have a good linear correlation with depth ($R2=0.9921$). It means that accumulation rate was consistent whether during strong EAWM or weak EAWM. Usually, strong EAWM would result in a higher accumulation. Why is accumulation rate consistent? Did the episodic erosion affect it (e.g., Stevens et al., 2018)?

Stevens, T., Buylaert, J.P., Thiel, C., et al., 2018. Ice-volume-forced erosion of the Chinese Loess Plateau global Quaternary stratotype site. Nature Communications, 9, 983.

Reply: We agree with the reviewer's point that the sedimentation rate is related to the EAWM intensity. However, DDW is a terrace sequence dominated by aeolian input, the supply of sediment for these deposits on terraces is comparatively abundant in the basin. These deposits are mainly transported by wind from short-distance sources (Liu et al., 2018). So the dust input are continuous whether EAWM is strong or weak. Furthermore, the grain-size distribution of DDW samples are different from those typical aeolian sediments on CLP. The values of mean grain size also exhibit large fluctuations.

4. Line 133: A space character before "µm" should be added.

5. Line 134: The space character between "µ" and "m" should be deleted.

6. Line 194, 222 and 253: "Zr/Br" should be "Zr/Rb".

7. The authors should add "δ" before "18O" in whole manuscript.

8. The reference style should be consistent. For example, in Line 292, "2.1-2.49" is incorrect. In Line 297, "24:" should be "24,".

Reply: All corrected.

References

An, Z.S., Colman, S.M., Zhou, W.J., Li, X.Q., Brown, E.T., Jull, A.J.T., Cai, Y.J., Huang, Y.S., Lu, X.F., Chang, H., Song, Y.G., Sun, Y.B., Xu, H., Liu, W.G., Jin, Z.D., Liu, X.D., Cheng, P., Liu, Y., Ai, L., Li, X.Z., Liu, X.J., Yan, L.B., Shi, Z.G., Wang, X.L., Wu, F., Qiang, X.K., Dong, J.B., Lu, F.Y., and Xu, X.W.: Interplay between the Westerlies and Asian monsoon recorded in Lake Qinghai sediments since 32 ka, Scientific Reports, 2, 619, 2012.

Berger, A.: Long term variations of daily insolations and quaternary climatic changes, Journal of the Atmospheric Sciences, 35, 2362-2367, 1978.

Caley, T., Roche, D.M., and Renssen, H.: Orbital Asian summer monsoon dynamics revealed using an isotope-enabled global climate model. Nature communications, 5: 5371, 2014.

Chen, F., Xu, Q., Chen, J., Birks, H.J.B., Liu, J., Zhang, S., Jin, L., An, C., Telford, R.J., Cao, X., Wang, Z., Zhang, X., Selvaraj, K., Lu, H., Li, Y., Zheng, Z., Wang, H., Zhou, A., Dong, G., Zhang, J., Huang, X., Bloemendal, J., and Rao, Z.: East Asian summer monsoon precipitation variability since the last deglaciation, Scientific Reports, 5, 11186, 2015.

Chen, J.H., Rao, Z.G., Liu, J.B., Huang, W., Feng, S., Dong, G.H., Hu, Y., Xu, Q.H., Chen, F.H.: On the timing of the East Asian summer monsoon maximum during the Holocene—Does the speleothem oxygen isotope record reflect monsoon rainfall variability?. Science China Earth Sciences, 59(12): 2328-2338, 2016.

Ding, Z.L., Xiong, S.F., Sun, J.M., Yang, S.L., Gu, Z.Y., and Liu, T.S.: Pedostratigraphy and paleomagnetism of a ~7.0 Ma eolian loess - red clay sequence at Lingtai, Loess Plateau, north-central China and the implications for paleomonsoon evolution. Palaeogeography, Palaeoclimatology, Palaeoecology, 152(1-2): 49-66, 1999.

Dykoski, C.A., Edwards, R.L., Cheng, H., Yuan, D.X., Cai, Y.J., Zhang, M.L., Liu, Y.S., Qing, J.M., An, Z.S., and Revenaugh, J.: A high-resolution, absolute-dated Holocene and deglacial Asian monsoon record from Dongge cave, China. Earth and Planetary Science Letters, 233 (1), 71-86, 2005.

Liu, J.B., Chen, J.H., Zhang, X.J., Li, Y., Rao, Z.G., and Chen, F.H.: Holocene East Asian summer monsoon records in northern China and their inconsistency with Chinese stalagmite δ18O records. Earth-Science Reviews, 148: 194-208, 2015.

Liu, J.B., Rühland, K. M., Chen, J. H., Xu, Y. Y., Chen, S. Q., Chen, Q. M., Huang, W., Xu, Q. H., Chen, F. H., and Smol, J. P.: Aerosol-weakened summer monsoons decrease lake fertilization in the Chinese Loess Plateau. Nature Climate Change, 7, 190-194, 2017.

Liu, X.X., Sun, Y.B., Vandenberghe, J., Li, Y., and An, Z.: Palaeoenvironmental implication of grain-size compositions of terrace deposits on the western Chinese Loess Plateau, Aeolian Research, 32, 202-209, 2018.

Nugteren, G., and Vandenberghe, J.: Spatial climatic variability on the Central Loess Plateau (China) as recorded by grain size for the last 250 kyr. Global and Planetary Change, 41(3-4): 185-206, 2004.

Tan, M.: Circulation effect: response of precipitation δ18O to the ENSO cycle in monsoon regions of China. Climate Dynamics, 42(3-4): 1067-1077, 2014.

Wang, Y.J., Cheng, H., Edwards, R.L., He, Y., Kong, X., An, Z.S., Wu, J., Kelly, M.J., Dykoski, C.A., and Li, X.: The Holocene Asian monsoon: links to solar changes and North Atlantic climate, Science, 308, 854-857, 2005.

Centennial to millennial-scale monsoon changes since the last deglaciation linked to solar activities and North Atlantic cooling

Xingxing Liu[1,2*], Youbin Sun[1,2,3*], Jef Vandenberghe[4], Peng Cheng[1,3,5], Xu Zhang[6,7], Evan J Gowan[7], Gerrit Lohmann[7], Zhisheng An[1,2,3]

[1]State Key Laboratory of Loess and Quaternary Geology, Institute of Earth Environment, Chinese Academy of Sciences, Xi'an, 710061, China

[2]CAS Center for Excellence in Quaternary Science and Global Change, Chinese Academy of Sciences, Xi'an, 710061, China.

[3]Institute of Global Environmental Change, Xi'an Jiaotong University, Xi'an, 710049, China

[4]Institute of Earth Sciences, Vrije Universiteit, De Boelelaan 1085, 1081 HV Amsterdam, The Netherlands

[5]Xi'an AMS Center of IEECAS, And Shaanxi Provincial Key Laboratory of Accelerator Mass Spectrometry and Application, Xi'an, 710061, China

[6]Key Laboratory of Western China's Environmental Systems (Ministry of Education), College of Earth and Environmental Sciences, Lanzhou University, Lanzhou, 730000, China

[7]Alfred Wegener Institute Helmholtz Centre for Polar and Marine Research, Bussestrasse 24, D-27570 Bremerhaven, Germany

[*]Corresponding author: Xingxing Liu (liuxx@ieecas.cn) and Youbin Sun (sunyb@ieecas.cn)

Abstract

Rapid monsoon changes since the last deglaciation remain poorly constrained due to the scarcity of geological archives. Here we present a high-resolution scanning X-ray fluorescence (XRF) analysis of a 13.5-m terrace succession on the western Chinese Loess Plateau (CLP) to infer rapid monsoon changes since the last deglaciation. Our results indicate that Rb/Sr and Zr/Rb are sensitive indicators of chemical weathering and wind sorting, respectively, which are further linked to the strength of the East Asia summer monsoon (EASM) and the East Asia winter monsoon (EAWM). During the last deglaciation, two cold intervals of the Heinrich event 1 and Younger Dryas were characterized by intensified winter monsoon and weakened summer monsoon. The EAWM gradually weakened since the beginning of the Holocene, while the EASM remained steady till 9.9 ka and then grew stronger. Both the EASM and EAWM intensity were relatively weak during the middle Holocene, indicate a mid-Holocene climatic optimum. Rb/Sr and Zr/Rb exhibit an anti-phase relationship between the summer and winter monsoon changes on centennial timescale during 16~1 ka BP. Comparison of these monsoon changes with solar activity and North Atlantic cooling events reveals that both factors can lead to abrupt changes on the centennial timescale in the early Holocene. During the late Holocene, North Atlantic cooling became the major forcing of centennial monsoon events.

Keywords: Chinese Loess Plateau; East Asian summer monsoon; East Asian winter monsoon; Elemental ratios; Centennial to millennial variability; Solar activities; North Atlantic cooling

1 Introduction

The East Asian monsoon (EAM) is one of the most important atmospheric circulation systems linked to climate changes over high- and low-latitude regions of the Northern

Hemisphere (Ding, 1994). It consists of summer and winter monsoons (EASM and EAWM) with significantly seasonal changes in moisture transportation and wind direction. During the past three decades, variability of the rain-bearing EASM on millennial to centennial time scales has been investigated extensively from cave deposits (Dykoski et al., 2005; Wang et al., 2005; Cheng et al., 2016), loess sequences (An et al., 1991; Ding et al, 1995; Sun et al., 2006, 2016; Kang et al., 2018), lake sediments (Yancheva et al., 2007; An et al., 2012; Chen et al., 2015; Liu et al., 2016), marine sediments (Huang et al., 2011), and model simulations (Wen et al., 2016). These previous studies show a series of oscillations and/or abrupt events, such as the 4.2, 8.2, 9.2 and 10.3 ka events. These records suggest the summer monsoon variations are not only induced by changes in Northern Hemisphere summer insolation, but also strongly modulated by internal land-ocean-air interactions of the Earth-climate systems (e.g., An et al., 2015).

Unlike abundant proxies of the EASM variability, high-resolution records reflecting millennial to centennial EAWM variability are still sparse. Though various proxies from different paleoclimatic archives have been used to document EAWM evolution since the last deglaciation, great differences were observed on the inferred winter monsoon changes and forcing mechanisms (Yancheva et al., 2007; Huang et al., 2011; Wang et al., 2012; Li and Morrill, 2015; Kang et al., 2018) . There are four primary factors contribute to these conflicting records. First, the loess-paleosol record on the Chinese Loess Plateau (CLP) (Sun et al., 2012; Kang et al., 2018) or marine sediments from the South China Sea (Huang et al., 2011) are not of sufficiently high resolution to detect centennial to millennial EAWM changes due to relatively-low sedimentation rates. Second, the sensitivity of various archives and proxies to changes in the monsoon intensity is different (e.g., Yancheva et al., 2007; Huang et al., 2011; Kang et al., 2018). Some environmental proxies commonly show different amplitudes and timing of variation, likely reflecting the fact that they respond to different aspects of climate and environment (temperature, wind and precipitation). Third, the proxies used for the EAWM remains controversial, such as whether Titanium (Ti) in Huguang Maar Lake is a proxy for local hydrology or EAWM intensity (Yancheva et al., 2007; Zhang et al., 2007). Fourth, uncertain chronologies from diverse natural archives (e.g., loess, lake, and marine) may lead to timing mismatch on centennial timescales.

Wen et al. (2016) performed a set of long-term transient simulations that suggest the EASM and EAWM are anti-correlated on millennial timescales in response to North Atlantic meltwater forcing during the last 21 ka. However, there is still a lack of high-resolution proxies to support this modelling result. This hampers our understanding of the effects of external solar forcing and internal meltwater feedbacks (Li and Morrill, 2015; Wen et al., 2016). Though numerous studies have focused on the rapid climate changes on the EASM and EAWM since the last deglaciation, significant differences and asynchronous changes still exist (e.g., Wang et al., 2005; Yancheva et al., 2007; Huang et al., 2011; An et al., 2012; Chen et al., 2015). Therefore, it is crucial to investigate high-resolution, independent proxies with robust chronology of the summer and winter monsoon intensities in one single archive to improve our understanding of rapid monsoon changes and dynamics in particular the centennial to millennial variability and coherent forcing mechanisms.

In this study, we investigate a thick terrace succession on the western CLP to determine EAWM and EASM variability since the last deglaciation for the first time. Our results provide valuable insights into the relationship between the EAWM and EASM variability at centennial to millennial timescales using high-resolution (5-mm interval) elemental records obtained by X-ray fluorescence (XRF) core scanning. We compare the elemental ratios (Zr/Rb and Rb/Sr) with other paleo-records of abrupt monsoon changes to determine the links with external solar forcing and internal feedbacks.

2 Materials and Methods

The Dadiwan section (DDW, 35.02°N, 105.8°E, 1454 m a.s.l) in Qin’an County, Gansu Province is located on the first terrace of the Wei River on the western CLP (Fig. 1A). Fluvio-aeolian sediments are thick and widely deposited on river terraces of the Wei River and its tributaries in this area (Fig. 1B). From 1981 to 2010, the mean annual precipitation and mean annual temperature in Qin’an County is 507.3 mm and 10.4℃, respectively (Meteorological data come from the national daily dataset of surface weather profile provided by the National Meteorological Data Center, http://data.cma.cn/data/). Dadiwan is known as the oldest example and type site of the “Dadiwan cultural” or “Laoguantai cultural” complex, which is the westernmost expression of early millet agriculture in North China. Previous studies in Dadiwan area based on organic carbon and pollen revealed that the middle Holocene was the most humid interval since the last deglaciation (Feng et al., 2004). During April 2015, we retrieved a 13.5-m core using a hydraulic-static drilling rig with a dual-tube (outer and inner tubes) core barrel. The core recovery rate was almost 100%, though some cores were slightly compressed (Fig. 1C).

After splitting the cores into a working and archive half with a Geotek core splitter, the surface of the cores was carefully smoothed to reduce scanning errors caused by irregularities from core slicing (Fig. 1C). The split core surface was subsequently covered with a 4 μm Ultralene film during core logging in order to avoid contamination of the XRF detector window and to prevent desiccation of the core surface. The split cores were scanned every 5-mm using an Avaatech XRF core scanner at the Institute of Earth Environment, Chinese Academy of Sciences.

The elements measured range from Al to Fe in the periodic table were detected at an X-ray voltage of 10 kV, Co to Mo at 30 kV, and Te to Ba at 50 kV (Richter et al., 2006; Weltje and Tjallingii, 2008). On the basis of the processed model, we used the WinAxil and WinAxilBatch software to calculate the element counts (counts per second, CPS) as peak integrals and applied background subtraction. The quality of every single spectrum and peak integral can be easily checked with the χ^2 value (Van Espen et al., 1977). As the variation in element concentrations of loess can be related to grain size sorting and chemical weathering (Chen et al., 1999, 2006; Peng and Guo, 2001), three elements (Rb, Zr and Sr) with high concentrations and low analytical uncertainties which were detected at 30 kV are discussed in this study.

After core scanning, sub-samples were taken at contiguous 1-cm intervals. A total of 1350 sub-samples were obtained for grain size and magnetic susceptibility analyses (see Fig. 2 in Liu et al., 2018 for a detailed description). A rough chronology of the DDW section was established by acceleratormass spectrometer (AMS) ^{14}C dates based on five total organic carbon from bulk sediments (Liu et al., 2018). In this study, seven additional ^{14}C dates from bulk organic matter were obtained in order to get more reliable age control. The samples were pretreated with 1M HCl (2 hr, 60°C) to remove carbonate, and then were thoroughly rinsed with distilled water (Zhou et al., 2006). Pretreated samples and CuO powder were placed into 9-mm quartz tubes, evacuated to 1×10^{-5} Torr, and then combusted. The pure CO_2 was collected using liquid nitrogen and reduced to graphite for AMS dating. For the AMS analysis, the CO_2 was reduced to graphite using Zn/Fe catalytic reduction. All these selected 12 samples were analyzed using a 3MV tandem accelerator at the Xi’an accelerated mass spectroscopy center and calibrated using calib. 7.0.2 (Reimer et al., 2004).

3 Results

Based on soil structure, color, magnetic susceptibility and grain size, the 13.5-m DDW core can be divided lithologically into three sub-units from bottom to top: 13~13.5 m, fluvial sediments; 6~13 m, loess deposits; 0~6 m, paleosol interbedded with four weakly weathered paleosol layers (Fig. 2A). The 12 radiocarbon ages have a linear correlation with depth. This is consistent with a continuous sediment accumulation under a stable environment between 16~1 ka BP. The age-depth model is constructed using linear regression ($y=1.1465x+1.2546$, $R^2=0.9921$), x is the depth in m, y is the calculated age (cal ka BP) (Fig. 2B). Since the dating errors ranges from 24 to 53 years and our 1-cm sampling strategy yields a time resolution of about 12 year, it is reasonable to discuss centennial to millennial scale monsoon variations since the last deglaciation based on our high-resolution results.

The magnetic susceptibility displays a stepwise increase from ~$13.7\times10^{-8}m^3kg^{-1}$ below 6 m to 15.5~$138.6\times10^{-8}m^3kg^{-1}$ above 6 m, with maximum values at three strongly weathered soil layers (Fig. 2C). Mean grain size, however, exhibits a two-stage variability except for the lower 0.5-m fluvial sandy layers (not shown here because it goes off the scale) (Fig. 2D); The lower part (13.5~6 m) exhibits large fluctuations (7.9~121.3 μm) while the loess-paleosol alternations (6~0 m) show small fluctuations (6.4~28.8 μ m). Generally, high magnetic susceptibility corresponds to fine mean grain-size, but the abrupt MS increase around 6 m is different from the gradual fining of the mean grain size between 8.2~6.8 m.

Similar to variations of magnetic susceptibility and grain-size, Rb, Sr and Zr exhibit significant variability, with ranges of 3400~8827 cps for Rb (Fig. 2E), 7000~40000 cps for Sr (Fig. 2F), and 7000~30000 cps for Zr (Fig. 2G). Low Rb/Sr ratio values correspond to low magnetic susceptibility, with values in the range from 0.18 to 0.6, revealing distinct pedogenic weathering effects. (Fig. 2H). The variation of the Zr/Rb ratio ranges from 1.2 to 5.8. High Zr/Rb ratios occur where grain-size is coarse, suggesting grain-size sorting effects (Fig. 2I).

4 Discussion

4.1 EAM variability on orbital timescale since the last deglaciation

A number of elements (e.g. Al, Si, K, Ca, Ti, Fe, Mn, Rb, Zr, Sr) based on scanning XRF have been used to acquire information of past climatic and environmental changes (Richter et al., 2006; Liang et al., 2012; Sun et al., 2016). However, the interpretation of lighter elements data require careful consideration due to the instrument detection limits and analytical uncertainties (e.g. organic matter and water content) (Richter et al., 2006). Considering the sedimentary characteristics and geochemical behavior of Zr (commonly abundant in coarse-grained sediments and resistant to weathering), Rb (enriched in clay deposits, relatively stable) and Sr (easily mobilized during chemical weathering), the ratios of Zr/Rb can be an indicator of grain-size sorting and Rb/Sr is an indicator of chemical weathering (Chen et al., 1999, 2006; Peng and Guo, 2001). Previous studies demonstrated that grain size and magnetic susceptibility of loess-paleosol sequences have been widely used as proxies for winter and summer monsoon, respectively (An et al., 1991; Ding et al, 1995; Sun et al., 2006). Taking into account the ratios of Zr/Rb and Rb/Sr are highly consistent with grain-size and magnetic susceptibility (Fig. 2), we used Zr/Rb and Rb/Sr ratios as proxies for EAWM and EASM intensity, respectively.

The Zr/Rb and Rb/Sr ratios reveal significant millennium- to centennial-scale variability (Fig. 3). During the last deglaciation, the Zr/Rb ratio has large-amplitude, high-frequency fluctuations, in contrast to small-amplitude and low-frequency oscillations during the Holocene (Fig. 3B). The Rb/Sr ratio exhibits relatively small-amplitude fluctuations during the last deglaciation to early Holocene (16~10 ka BP) and mid-to-late Holocene (7-1 ka BP). In the early to mid-Holocene (10-7 ka BP), there are large amplitude fluctuations (Fig. 3C). During the last deglaciation, two cold intervals of the Heinrich event 1 (16~14.8 ka) and Younger Dryas (YD, 12.8~11.7 ka) were characterized by intensified EAWM (Fig. 3B) and weakened EASM (Fig. 3C). The period from 14.8~12.8 ka with strong EASM/weak EAWM, which might be temporally consistent with the Bølling-Allerød (BA) warming episode. A rapid weakening of the EAWM occurred during the early Holocene, and then reached a minimum during 9.9~4.8 ka in the middle Holocene (Fig. 3B). Minimum EASM intensity occurs from 11.7~9.9 ka during the early Holocene, and increased to the highest level during during 8~4.8 ka during the middle Holocene (Fig. 3C). In the late Holocene, a shift of the monsoon intensity is evident in both Zr/Br and Rb/Sr, EASM continue to moderate while EAWM increased gradually.

On orbital time scales, changes in the EAWM have been linked to changes in ice volume in the Northern Hemisphere (Ding et al., 1995; Liu and Ding, 1998; Porter, 2001). It has been shown that Northern Hemisphere ice sheets in land were larger during the early-middle Holocene than during the late Holocene (Dyke and Prest, 1987; Kutzbach et al., 1998). The winter insolation in Northern Hemisphere is lower during early Holocene than during late Holocene (Berger and Loutre, 1991). Such change in the size of ice sheets and the insolation should have caused a strengthening of the EAWM during the early Holocene. However, the intensity of EAWM appears to be different between the DDW and the Lake Huguang Maar (Fig. 3A) (Yancheva et al., 2007) in southern China during the early Holocene. This discrepancy might attribute to the ice sheets at high latitudes did not influence the EAWM over southern China as strongly as they influenced EAWM expression in northern China during the early Holocene.

Orbital trend of EASM intensity from DDW generally resembles the Pollen-based annual precipitation (PANN) reconstructed from Gonghai Lake (Fig.3D) (Chen et al., 2015; Liu et al., 2015, 2017), indicate a mid-Holocene climatic optimum (Liu et al., 2015). This suggests that EASM intensity not only follows changes in insolation inferred from the Lake Qinghai summer monsoon index (SMI) (Fig. 3E) (An et al., 2012) and stalagmite δ^{18}O records in eastern China (Fig. 3F) (Dykoski et al., 2005; Wang et al., 2005), but was also strongly moderated by the internal feedback processes such as continuous freshwater input into the North Atlantic caused by the remnant melting Laurentide ice sheet (Chen et al., 2015). In addition to this, asynchronous changes among these proxies can be possible due to varied sensitivity of these proxies and archives to changes in the monsoon intensity (Caley et al., 2014).

4.2 Centennial monsoon variability since the last deglaciation

EAWM and EASM intensity are anti-phase at both millennial- and centennial-scale since the last deglaciation (Fig. 3). That is, when the EAWM is strong, the EASM is weak. A series of strong EAWM and weak EASM events (e.g., H1, YD, 11.1, 10.1, 9.3, 8.2, 7.3, 6.7, 5.9, 4.6 and 2.1 ka) can be identified from Zr/ Rb and Rb/Sr values. The mechanism of this anti-phase relationship between EAWM and EASM on milliennial to centennial scale can potentially be ascribed to the release of meltwater into the North Atlantic and the resulted change in the Atlantic Meridional Overturning Circulation (AMOC) (Broecker et al., 1992; Alley et al., 1997; Bond et al., 2001; Wen et al., 2016). In addition, previous studies also suggest that the change in the solar activity partly influences EAWM/EASM strength in centennial timescale, through the the migration of annual mean position of the intertropical convergence zone (ITCZ) during summer times (Haug et al., 2001; Dykoskietal., 2005;Wang et al.,2005; Yancheva et al., 2007; Steinhilber et al.,2012), and changes in the meridional temperature gradient during winter times

(Xiao et al., 2006; Liu et al., 2009; Sagawa et al., 2014). However, some of the intervals (e.g., YD, 11.1, 6.7 ka) are more distinct in the Zr/Rb ratio, while some intervals such as the 7.3 ka event is more distinct in the Rb/Sr ratio. The differences between the two proxies records during these abrupt intervals shows that they have variable sensitivity to monsoonal wind and precipitation intensity changes (Sun et al., 2012; Chen et al., 2015).

The centennial-scale winter monsoon changes since the last deglaciation reconstructed at DDW are partially consistent with previous high-resolution Ti records from Lake Huguang Maar in southern China (Fig. 3A) (Yancheva et al., 2007). This support that the record of Ti counts can be a measure of winter monsoon strength although it is still controversial due to the provenance of the lake sediments (Yancheva et al., 2007; Zhang et al., 2007). Some of the strong winter monsoon intervals (e.g., 7.3 ka) are not significant in the Lake Huguang Maar, which indicate that DDW, located in northern China, is more sensitive to the EAWM system. Another possibility for this discrepancy is that control points between 8 ka and 4ka are lacking in the Lake Huguang Maar (Fig. 3A).

Compared with other summer monsoon proxy records in China, the centennial-scale EASM changes at DDW are consistent with the PANN reconstructed from Gonghai Lake (Fig.3D) (Chen et al., 2015; Liu et al., 2015, 2017) and SMI from Lake Qinghai (Fig. 3E) (An et al., 2012). Almost all the weak summer monsoon intervals, within dating errors, appear to coincide with major changes in the PANN reconstruction and SMI. It is worth noting that 8.2 ka event was not significant in the Gonghai (Fig. 3D) and Qinghai Lake (Fig. 3E). This could be ascribed to age model discrepancies, or the variable sensitivity of different proxies to changes in monsoon intensity (Chen et al., 2015). However, there are some discrepancies between Rb/Sr ratio of DDW and the and $\delta^{18}O$ record from Dongge Cave stalagmites in eastern China (Fig. 3F)

(Dykoski et al., 2005; Wang et al., 2005). This discrepancy might attribute to the controversial paleoclimatic significance of δ^{18}O records from caves in southern China, or the North-South differences for the monsoon intensity (Caley et al., 2014; Tan, 2014; Liu et al., 2015; Chen et al., 2016). Therefore, the weak EASM intervals existing in all these three different regions (CLP, northeast of Tibetan Plateau and eastern China) may have recorded centennial EASM variability since the last deglaciation.

4.3 Links between solar forcing and high-latitude climate changes

We removed the long-term trend of Zr/Rb and Rb/Sr ratios to investigate the high frequency components of the signal (<1 kyr), then compare the results with the North Atlantic hematite-stained grains records (HSG) (Bond et al., 2001) and atmospheric ^{14}C production rate (△^{14}C) (Reimer et al., 2013) (Fig. 4a). HSG is a tracer of drift ice in the North Atlantic, high values of HSG indicate cold conditions (Bond et al., 2001). Higher values of atmospheric △^{14}C represent weak solar activity and vice versa (Stuiver and Quay, 1980). High-frequency components of the EAWM (Fig. 4B) and EASM (Fig. 4C) proxies from DDW exhibit large-amplitude fluctuations during the early Holocene (11.5~7 ka), while the amplitude variations were more moderate during the late Holocene (7~1 ka), especially the Rb/Sr ratio. All the strong winter and weak summer monsoon intervals from DDW records can either be correlated with HSG (Fig. 4A), or with high atmospheric △^{14}C (Fig. 4D). This indicate possible relationship with Northern Hemisphere cooling and solar activity.

During the early Holocene (11.5~7 ka), all of the strong EAWM/weak EASM intervals (e.g., 11.1, 10.1, 9.3, 8.2, 7.3 ka BP) within the limits of dating error are correlated with HSG (Fig. 4A) and high △^{14}C (Fig. 4D). High similarity of these records suggests that the North Atlantic cooling events and solar activity probably simultaneously affect the EAM systems on centennial timescales. During the late Holocene (7~1 ka), all the strong EAWM (Fig. 4B) and weak EASM (Fig. 4C) events (e.g., 6.7, 5.9, 4.6, 3.3, 2.8 and 2.1 ka BP) correspond well to the abrupt events in the North Atlantic region. This indicates that North Atlantic cooling plays an important role in driving the centennial monsoon changes during the late Holocene. The 3.3 and 2.8 ka events are also correlated well with high $\triangle^{14}$C, which indicate solar forcing also plays a role during those times.

In order to further confirm the possible link of monsoon variability with internal North Atlantic feedbacks and external solar forcing on centennial-scale, spectral analyses were conducted on these proxies for the early (11.5~7 ka) (Fig. 4b) and late (7~1 ka) (Fig. 4c) Holocene (Fig. 4). The spectral results reveal that the Zr/Rb and Rb/Sr records both display a prominent periodicity at 1.0 kyr (Fig. 4F and G). This matches with the cycle of HSG (Fig. 4E) and $\triangle^{14}$C (Fig. 4H) during the early Holocene. The similarity in periodicity further confirm the link of centennial EAM variability to North Atlantic cooling and solar activities during the early Holocene (11.5~7 ka). However, the dominant periodicity (~1.27 kyr) of HSG, Zr/Rb and Rb/Sr records are not evident in the $\triangle^{14}$C spectrum during the late Holocene (7~1 ka) (Fig.4I-L), implying that solar forcing is not the dominant cause of centennial monsoon variability during this period.

North Atlantic cooling and solar activity are two commonly accepted drivers of centennial climate variability. There is a teleconnection between rapid monsoon changes and abrupt events in the North Atlantic region (the ocean thermohaline circulation) (Broecker et al., 1992; Alley et al., 1997; Bond et al., 2001; Wang et al., 2005). The strength of the Siberian High, located north of our DDW section, increases when the North Atlantic is in a cold mode (Gong et al., 2001).

The ITCZ shifted southward due to changes in the AMOC and temperature gradients across the northern hemisphere. When ITCZ shifted southward, the EASM weakened and EAWM strengthened (Broccoli et al., 2006; Sun et al., 2012; Wen et al., 2016). Speleothem records from China (Dykoski et al., 2005; Cheng et al., 2006; Wang et al., 2008) and many model simulations (Chiang and Bitz 2005; Broccoli et al. 2006) support this.

The change in solar activity could contribute to the regional monsoon variability by affecting low-latitude hydrological processes (Liu et al. 2009; Yan et al. 2015). Specifically, decreased summer insolation results in changes to the land-ocean thermal contrast. The sea surface temperature in the western tropical Pacific decreases and the Northwest Pacific Subtropical High weakens (Liu et al., 2003; Cai et al., 2010). This decreased thermal contrast would result in a southward migration of the ITCZ and also weaken the EASM strength by reducing the monsoon moisture transport from the tropical ocean to the continent in low latitudes (Liu et al. 2009; Yan et al. 2015). Since changes in solar output are large at centennial-scale during the early Holocene, this may amplify the solar output effect due to nonlinear responses and feedback processes of the climate system (Mohtadi et al., 2016). During the late Holocene (7~1 ka), there is a decrease of summer insolation and the small-amplitude fluctuations of solar activities (Fig. 4D) (Berger, 1978). This is probably why it play a less important role in EAM system.

5 Conclusions

We recovered a high-resolution last deglaciation record of EAWM and EASM from terrace sediments on the western CLP. Ratios of Zr/Rb and Rb/Sr are sensitive indicators of winter wind intensity and chemical weathering, respectively, and thus can be regarded as an index of EAWM and EASM. In general, the ratios of Rb/Sr and Zr/Rb display significant fluctuation similar to the global climate characteristics since the last deglaciation (16~1 ka BP), such as Heinrich cooling (H1), Bølling-Allerød warming, and Younger Dryas cooling events. Both EAWM and EASM show “Holocene optimum” during the middle Holocene. A number of strong and weak monsoon changes are identified by means of Zr/Rb and Rb/Sr values from DDW, such as strong EAWM/weak EASM intervals around H1, YD, 11.1, 10.1, 9.3, 8.2, 5.9, 4.6, 3.3, 2.8 and 2.1 ka, which reveals a negative co-variabiltiy between the EAWM and EASM on centennial timescale. Our Zr/Rb and Rb/Sr records are consistent with the Ti content from Lake Huguang Maar (EAWM proxy), the PANN reconstructed from Gonghai Lake and the SMI from Lake Qinghai (both EASM proxies). Comparing with North Atlantic cooling and solar activity proxies, our record shows that both are possible driving factors of centennial monsoon variability. North Atlantic cooling events and solar activity are the dominant forcing of the EAM system during the early Holocene, while North Atlantic cooling became more important during the late Holocene.

Data availability

All data are accessible from the authors. Correspondence and requests for materials should be addressed to Xingxing Liu (liuxx@ieecas.cn).

Author contributions

Xingxing Liu and Youbin Sun designed the study and performed the fieldwork and experiments. Jef Vandenberghe, Xu Zhang contributed to data analysis. Peng Cheng conducted the AMS ^{14}C analysis. Evan J Gowan, Gerrit Lohmann and Zhisheng An improved the manuscript with their contributions.

Competing interests

The authors declare that they have no conflict of interest.

Acknowledgments

This work was supported by The National Key Research and Development Program of China (2016YFA0601902), the National Science Foundation of China (41807425 and 41525008), and the Open Foundation of State Key Laboratory of Loess and Quaternary Geology (SKLLQG1633).

References

Alley, R.B., Mayewski, P.A., Sowers, T., Stuiver, M., Taylor, K.C., and Clark, P.U.: Holocene climatic instability: A prominent, widespread event 8200 yr ago, Geology, 25 (6), 483-486, 1997.

An, Z.S., Colman, S.M., Zhou, W.J., Li, X.Q., Brown, E.T., Jull, A.J.T., Cai, Y.J., Huang, Y.S., Lu, X.F., Chang, H., Song, Y.G., Sun, Y.B., Xu, H., Liu, W.G., Jin, Z.D., Liu, X.D., Cheng, P., Liu, Y., Ai, L., Li, X.Z., Liu, X.J., Yan, L.B., Shi, Z.G., Wang, X.L., Wu, F., Qiang, X.K., Dong, J.B., Lu, F.Y., and Xu, X.W.: Interplay between the Westerlies and Asian monsoon recorded in Lake Qinghai sediments since 32 ka, Scientific Reports, 2, 619, 2012.

An, Z.S., Kukla, G., Porter, S.C., and Xiao, J.L.: Late Quaternary dust flow on the Chinese loess plateau, Catena, 18 (2), 125-132, 1991

An, Z.S., Wu, G.X., Li, J.P., Sun, Y.B., Liu, Y.M., Zhou, W.J., Cai, Y.J., Duan, A.M., Li, L., Mao, J.Y., Cheng, H., Shi, Z.G., Tan, L.C., Yan, H., Ao, H., Chang, H., and Juan, F.: Global Monsoon Dynamics and Climate Change, Annu. Rev. Annual Review of Earth and Planetary Sciences, 43, 29-77, 2015.

Berger, A.: Long term variations of daily insolations and quaternary climatic changes, Journal of the Atmospheric Sciences, 35, 2362-2367, 1978.

Berger, A., and Loutre, M.F.: Insolation values for the climate of the last 10 million years. Quaternary Science Reviews, 10(4): 297-317, 1991.

Berntsson, A., Rosqvist, G.C., and Velle, G.: Late-Holocene temperature and precipitation changes in Vindelfjällen, mid - western Swedish Lapland, inferred from chironomid and geochemical data, The Holocene, 24, 78-92. doi: 10.1177/0959683613512167, 2014.

Bond, G., Kromer, B., Beer, J., Muscheler, R., Evans, M.N., Showers,W., Hoffmann, S., Lotti Bond, R., Hajdas, I., and Bonani, G.: Persistent solar influence on North Atlantic climate during the Holocene, Science, 294 (5549), 2130-2136, 2001.

Broccoli, A. J., Dahl, K. A., and Stouffer, R. J.: Response of the ITCZ to Northern Hemisphere cooling, Geophysical Research Letters, 33(1), 2006.

Broecker, W., Bond, G., Klas, M., Clark, E., and McManus, J.: Origin of the northern Atlantic's Heinrich events, Climate Dynamics, 6 (3-4), 265-273, 1992.

Cai, Y.J., Tan, L.C., Cheng, H., An, Z.S., Edwards, R.L., Kelly, M.J., Kong, X.G.,and Wang, X.F.: The variation of summer monsoon precipitation in Central China since the last deglaciation, Earth and Planetary Science Letters, 291 (1), 21-31, 2010.

Caley, T., Roche, D.M., and Renssen, H.: Orbital Asian summer monsoon dynamics revealed using an isotope-enabled global climate model. Nature communications, 5: 5371, 2014.

Chen, F., Xu, Q., Chen, J., Birks, H.J.B., Liu, J., Zhang, S., Jin, L., An, C., Telford, R.J., Cao, X., Wang, Z., Zhang, X., Selvaraj, K., Lu, H., Li, Y., Zheng, Z., Wang, H., Zhou, A., Dong, G., Zhang, J., Huang, X., Bloemendal, J., and Rao, Z.: East Asian summer monsoon precipitation variability since the last deglaciation, Scientific Reports, 5, 11186, 2015.

Chen, J., An, Z.S., Wang, Y.J., Ji, J.F., Chen, Y., and Lu, H.Y.: Distribution of Rb and Sr in the Luochuan loess-paleosal sequence of China during the last 800 kaimplications for paleomonsoon variations, Science China Earth Sciences, 42, 225-232, 1999.

Chen, J., Chen, Y., Liu, L., Ji, J., Balsam, W., Sun, Y., and Lu, H.: Zr/Rb ratio in the Chinese loess sequences and its implication for changes in the East Asian winter monsoon strength, Geochimica et Cosmochimica Acta, 70, 1471-1482, 2006.

Chen, J.H., Rao, Z.G., Liu, J.B., Huang, W., Feng, S., Dong, G.H., Hu, Y., Xu, Q.H., Chen, F.H.: On the timing of the East Asian summer monsoon maximum during the Holocene—Does the speleothem oxygen isotope record reflect monsoon rainfall variability?. Science China Earth Sciences, 59(12): 2328-2338, 2016.

Cheng, H., Edwards, R. L., Wang, Y., Kong, X., Ming, Y., Kelly, M. J., Wang, X.F., Gallup, C.D., and Liu, W.G.: A penultimate glacial monsoon record from Hulu Cave and two-phase glacial terminations, Geology, 34(3), 217-220, 2006.

Cheng, H., Edwards, R.L., Sinha, A., Spotl, C., Yi, L., Chen, S.T., Kelly, M., Kathayat, G., Wang, X.F., Li, X.L., Kong, X.G.,Wang, Y.J., Ning, Y.F., and Zhang, H.W.: The Asian monsoon over the past 640,000 years and ice age terminations, Nature, 534, 640-646, 2016.

Chiang, J.C.H., and Bitz, C.M.: Influence of high latitude ice cover on the marine Intertropical Convergence Zone, Climate Dynamics, 25, 477-496, 2005.

Ding, Y.H.: Monsoon over China, Kluwer Academic, p. 420, 1994.

Ding, Z.L., Liu, T.S., Rutter, N.W., Yu, Z.W., Guo, Z.T., and Zhu, R.X.: Ice-volume forcing of East Asian winter monsoon variations in the past 800,000 years, Quaternary Research, 44 (2), 149-159, 1995.

Dyke, A., and Prest, V.: Late Wisconsinan and Holocene history of the Laurentide ice sheet[J]. Géographie physique et Quaternaire, 41(2): 237-263, 1987.

Dykoski, C.A., Edwards, R.L., Cheng, H., Yuan, D.X., Cai, Y.J., Zhang, M.L., Liu, Y.S., Qing, J.M., An, Z.S., and Revenaugh, J.: A high-resolution, absolute-dated Holocene and deglacial Asian monsoon record from Dongge cave, China. Earth and Planetary Science Letters, 233 (1), 71-86, 2005.

Feng, Z.D., An, C.B., Tang, L.Y., and Jull, A.J.T.: Stratigraphic evidence of a Megahumid climate between 10,000 and 4000 years BP in the western part of the Chinese Loess Plateau, Global and Planetary Change, 43 (3), 145-155, 2004.

Gong, D.Y., Wang, S.W., and Zhu, J.H.: East Asian winter monsoon and Arctic Oscillation, Geophysical Research Letters, 28 (10), 2073-2076, 2001.

Haug, G.H., Hughen, K.A., Sigman, D.M., Peterson, L.C., and Röhl, U.: Southward migration of the intertropical convergence zone through the Holocene. Science, 293(5533): 1304-1308, 2001.

Huang, E., Tian, J., and Steinke, S.: Millennial-scale dynamics of the winter cold tongue in the southern South China Sea over the past 26 ka and the East Asian winter monsoon, Quaternary Research, 75 (1), 196-204, 2011.

Kang, S.G., Wang, X.L., Roberts, H. M., Duller, G. A., Cheng, P., Lu, Y.C., and An, Z.S.: Late Holocene anti-phase change in the East Asian summer and winter monsoons, Quaternary Science Reviews, 188, 28-36, 2018.

Kutzbach, J., Gallimore, R., Harrison, S., Behlinga, P., Selina, R., and Laarif, F.: Climate and biome simulations for the past 21,000 years. Quaternary Science Reviews, 17(6-7): 473-506, 1998.

Li, Y., and Morrill, C.: A Holocene East Asian winter monsoon record at the southern edge of the Gobi Desert and its comparison with a transient simulation, Climate Dynamics, 45, 1219-1234, 2015.

Liang, L.J., Sun, Y.B., Yao, Z.Q., Liu, Y.G., and Wu, F.: Evaluation of high-resolution elemental analyses of Chinese loess deposits measured by X-ray fluorescence core scanner, Catena, 92: 75-82, 2012.

Liu, J., Wang, B., Ding, Q., Kuang, X., Soon, W., and Zorita, E.: Centennial variations of the global monsoon precipitation in the last millennium: results from ECHO-G model, Journal of Climate, 22:2356-2371, 2009.

Liu, J.B., Chen, J.H., Zhang, X.J., Li, Y., Rao, Z.G., and Chen, F.H.: Holocene East Asian summer monsoon records in northern China and their inconsistency with Chinese stalagmite δ^{18}O records. Earth-Science Reviews, 148: 194-208, 2015.

Liu, J. B., Rühland, K. M., Chen, J. H., Xu, Y. Y., Chen, S. Q., Chen, Q. M., Huang, W., Xu, Q. H., Chen, F. H., and Smol, J. P.: Aerosol-weakened summer monsoons decrease lake fertilization in the Chinese Loess Plateau. Nature Climate Change, 7, 190-194, 2017.

Liu, T., and Ding, Z.: Chinese loess and the paleomonsoon. Annual review of earth and planetary sciences, 26(1): 111-145, 1998.

Liu, X.Q., Dong, H.L., Yang, X.D.,Herzschuh, U., Zhang, E.L., W.Stuut, J., and Wang, Y.B.: Late Holocene forcing of the Asian winter and summer monsoon as evidenced by proxy records from the northern Qinghai-Tibetan Plateau. Earth and Planetary Science Letters, 280(1-4): 276-284, 2009.

Liu, X.X., Sun, Y.B., Vandenberghe, J., Li, Y., and An, Z.: Palaeoenvironmental implication of grain-size compositions of terrace deposits on the western Chinese Loess Plateau, Aeolian Research, 32, 202-209, 2018.

Liu, X.X., Vandenberghe, J., An, Z.S., Li, Y., Jin, Z.D., Dong, J.B., and Sun, Y.B.: Grain size of Lake Qinghai sediments: implications for riverine input and Holocene monsoon variability, Palaeogeography, Palaeoclimatology, Palaeoecology, 449, 41-51, 2016.

Liu, Z., Otto-Bliesner, B., Kutzbach, J., Li, L., and Shields, C.: Coupled climate simulation of the evolution of global monsoons in the Holocene, Journal of Climate, 16(15), 2472-2490, 2003.

Mohtadi, M., Prange, M., and Steinke, S.: Palaeoclimatic insights into forcing and response of monsoon rainfall, Nature, 533, 191-199, 2016.

Peng, S.Z., and Guo, Z.T.: Geochemical indicator of original eolian grain size and implications on winter monsoon evolution, Science in China Series D: Earth Sciences, 44: 261-266, 2001.

Porter, S. C.: Chinese loess record of monsoon climate during the last glacial–interglacial cycle. Earth-Science Reviews, 54(1-3): 115-128, 2001.

Rasmussen, S.O., Andersen, K.K., Svensson, A.M., Steffensen, J.P., Vinther, B.M., Clausen, H.B., Siggaard-Andersen, M.L., Johnsen, S.J., Larsen, L.B., Dahl-Jensen, D., Bigler, M., Röhlisberger, R., Fischer, H., Goto-Azuma, K., Hansson, M.E., and Ruth, U.: A new Greenland ice core chronology for the last glacial termination, Journal of Geophysical Research: Atmospheres, 111(D6), 2006.

Reimer, P.J., Baillie, M.G.L., Bard, E., Bayliss, A., Beck, J.W., Bertrand, C.J.H., Blackwell, P.G., Buck, C.E., Burr, G.S., Cutler, K.B., Damon, P.E., Edwards, R.L., Fairbanks, R.G., Friedrich, M., Guilderson, T.P., Hogg, A.G., Hughen, K.A., Kromer, B., McCormac, G., Manning, S., Ramsey, C.B., Reimer, R.W., Remmele, S., Southon, J.R., Stuiver, M., Talamo, S., Taylor, F.W., van der Plicht, J., and Weyhenmeyer, C.E.: IntCal04 terrestrial radiocarbon age calibration, 0-26 cal kyr BP, Radiocarbon, 46 (3), 1029-1058, 2004.

Reimer, P.J., Bard, E., Bayliss, A., Beck, J.W., Blackwell, P.G., Bronk Ramsey, C., Buck, C.E., Cheng, H., Edwards, R.L., and Friedrich, M.: IntCal13 and Marine13 radiocarbon age calibration curves 0-50,000 years cal BP, Radiocarbon, 55, 1869-1887, 2013.

Richter, T. O., Van der Gaast, S., Koster, B., Vaars, A., Gieles, R., de Stigter, H. C., Haas, H.D., and van Weering, T. C.: The Avaatech XRF Core Scanner: technical description and applications to NE Atlantic sediments, Geological Society, London, Special Publications, 267(1), 39-50, 2006.

Sagawa, T., Kuwae. M., Tsuruoka, K., Nakamura, Y., Ikehara, M., and Murayama, M.: Solar forcing of centennial-scale East Asian winter monsoon variability in the mid-to late Holocene. Earth and Planetary Science Letters, 395: 124-135, 2014.

Shala, S., Helmens, K., Jansson, K., Kylander, M., Risberg, J., and Lowemark, L.: Palaeoenvironmental record of glacial lake evolution during the early Holocene at Sokli, NE Finland, Boreas, 43: 362-376. doi: 10.1111/bor.12043, 2014.

Steinhilber, F., Beer, J., and Fröhlich, C.: Total solar irradiance during the Holocene[J]. Geophysical Research Letters, 36(19), 2009.

Stuiver, M., and Quay, P.D.: Changes in atmospheric carbon-14 attributed to a variable sun, Science, 207 (4426), 11-19, 1980.

Sun, Y.B., Chen, J., Clemens, S.C., Liu, Q.S., Ji, J.F., and Tada, R.: East Asian monsoon variability over the last seven glacial cycles recorded by a loess sequence from the northwestern Chinese Loess Plateau, Geochemistry, Geophysics, Geosystems, 7 (12), 2006.

Sun, Y.B., Clemens, S.C., Morrill, C., Lin, X.P., Wang, X.L., and An, Z.S.: Influence of Atlantic meridional overturning circulation on the East Asian winter monsoon, Nature Geoscience, 5 (1), 46-49, 2012.

Sun, Y.B., Liang, L.J., Bloemendal, J., Li, Y., Wu, F., Yao, Z.Q., and Liu, Y.G.: High‐resolution scanning XRF investigation of Chinese loess and its implications for millennial‐scale monsoon variability, Journal of Quaternary Science, 31(3), 191-202, 2016.

Tan, M.: Circulation effect: response of precipitation $\delta^{18}O$ to the ENSO cycle in monsoon regions of China. Climate Dynamics, 42(3-4): 1067-1077, 2014.

Van Espen, P., Nullens, H., and Adams, F.: A computer analysis of X-ray fluorescence spectra, Nuclear Instruments and Methods, 142(1-2), 243-250, 1977.

Wang, L., Li, J.J., Lu, H.Y., Gu, Z.Y., Rioual, P., Hao, Q.Z., Mackay, A.W., Jiang, W.Y., Cai, B.G., Xu, B., Han, J.T., and Chu, G.Q.: The East Asian winter monsoon over the last 15,000 years: its links to high-latitudes and tropical climate systems and complex correlation to the summer monsoon, Quaternary Science Reviews, 32, 131-142, 2012.

Wang, Y.J., Cheng, H., Edwards, R.L., He, Y., Kong, X., An, Z.S., Wu, J., Kelly, M.J., Dykoski, C.A., and Li, X.: The Holocene Asian monsoon: links to solar changes and North Atlantic climate, Science, 308, 854-857, 2005.

Weltje, G. J., and Tjallingii, R.: Calibration of XRF core scanners for quantitative geochemical logging of sediment cores: theory and application, Earth and Planetary Science Letters, 274(3-4), 423-438, 2008.

Wen, X.Y., Liu, Z.Y., Wang, S.W., Cheng, J., and Zhu, J.: Correlation and anticorrelation of the East Asian summer and winter monsoons during the last 21,000 years, Nature Communications, 7, 11999, 2016.

Xiao. S.B., Li, A.C., Liu, J.P., Chen, M.H., Xie, Q., Jiang, F.Q., Li, T.G., Xiang, R., and Chen, Z.: Coherence between solar activity and the East Asian winter monsoon variability in the past 8000 years from Yangtze River-derived mud in the East China Sea. Palaeogeography, Palaeoclimatology, Palaeoecology, 237(2-4): 293-304, 2006.

Yan, H., Soon,W., and Wang, Y.: A composite sea surface temperature record of the northern South China Sea for the past 2500 years: a unique look into seasonality and seasonal climate changes during warm and cold periods, Earth-Science Reviews, 141, 122-135, 2015.

Yancheva, G., Nowaczyk, N.R., Mingram, J., Dulski, P., Schettler, G., Negendank, J.F.W., Liu, J., Sigman, D.M., Peterson, L.C., and Haug, G.H.: Influence of the intertropical convergence zone on the East Asian monsoon, Nature, 445, 74-77, 2007.

Zhang, D. E., and Lu, L.: Anti-correlation of summer/winter monsoons?. Nature, 450(7168), E7, 2007.

Zhou, W.J., Zhao, X.L., Lu, X.F., Liu, L., Wu, Z.K., Cheng, P., Zhao, W.N., and Huang, C.H.: The 3MV multi-element AMS in Xi'an, China: unique features and preliminary tests, Radiocarbon, 48(2), 285-293, 2006.

Figures

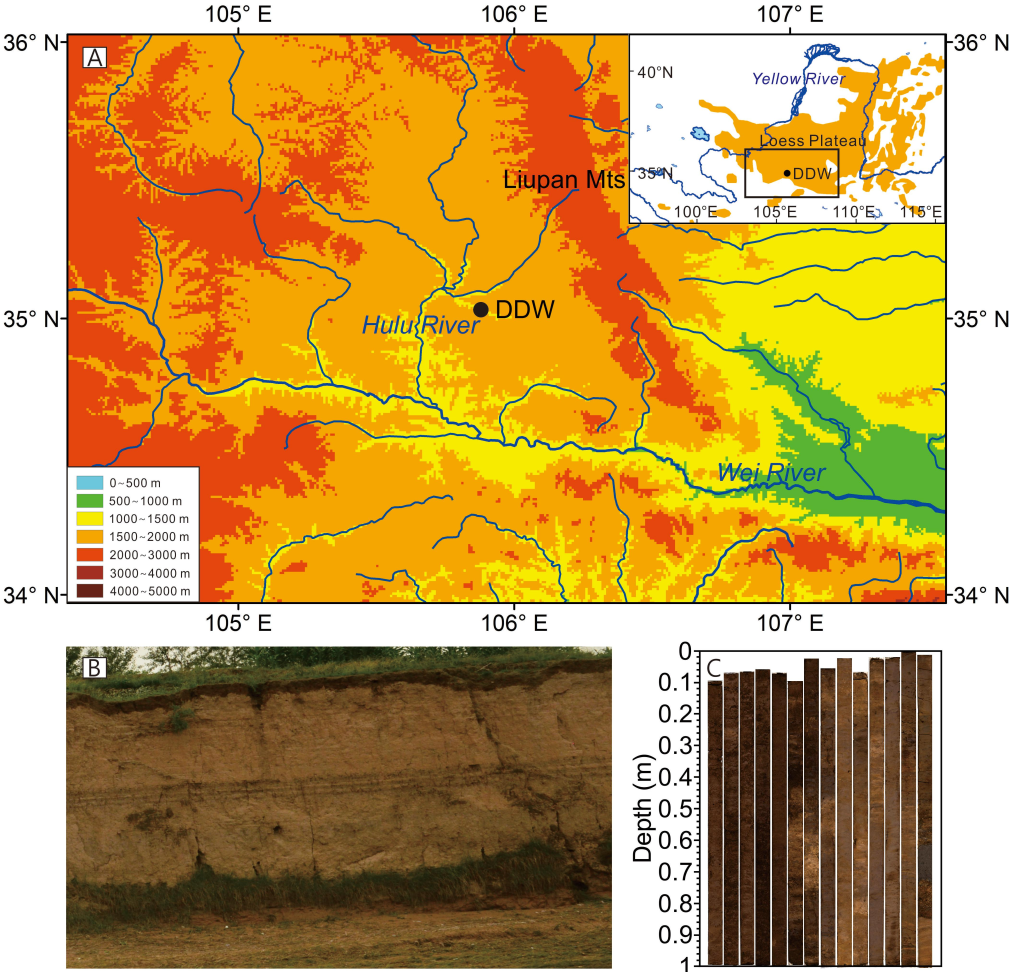

Fig 1. Map showing the CLP and location of the DDW (A), photographs of DDW terrace outcrop (B) and cores (C).

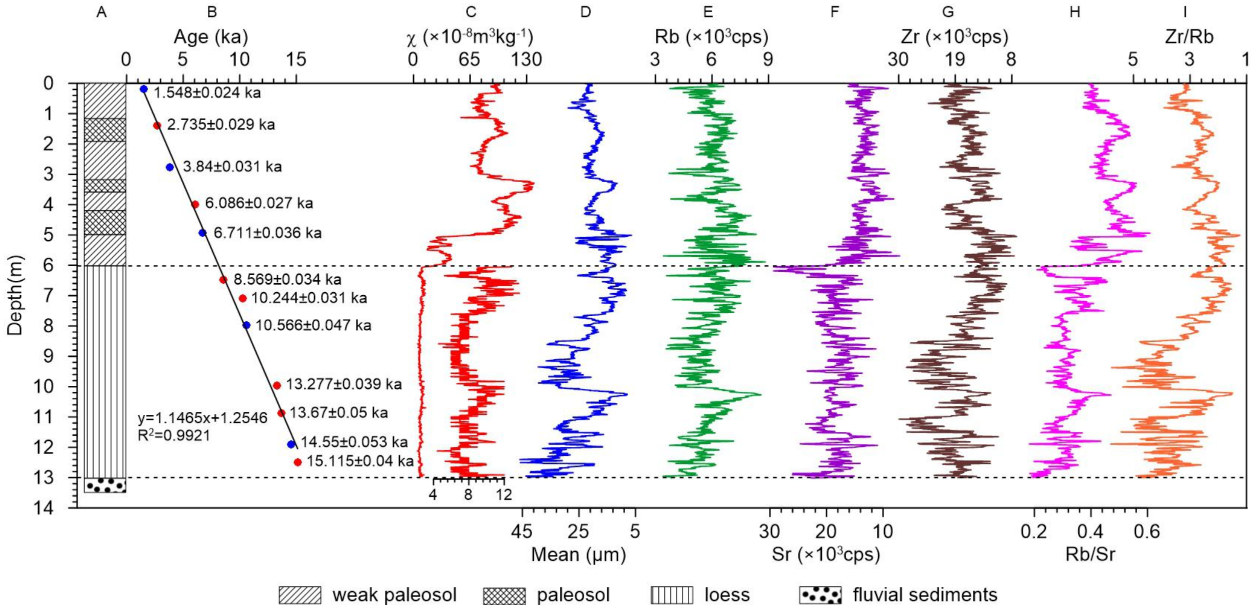

Fig 2. Stratigraphy (A), age-depth model (B), magnetic susceptibility (C), grain-size results (D) and elemental results (E, F, G, H, I) measured by scanning XRF of the DDW core. Five red dots are ages in previous work (Liu et al., 2018). Blue dots are seven additional ages in this study. The elemental results were smoothed with a 3-point moving average.

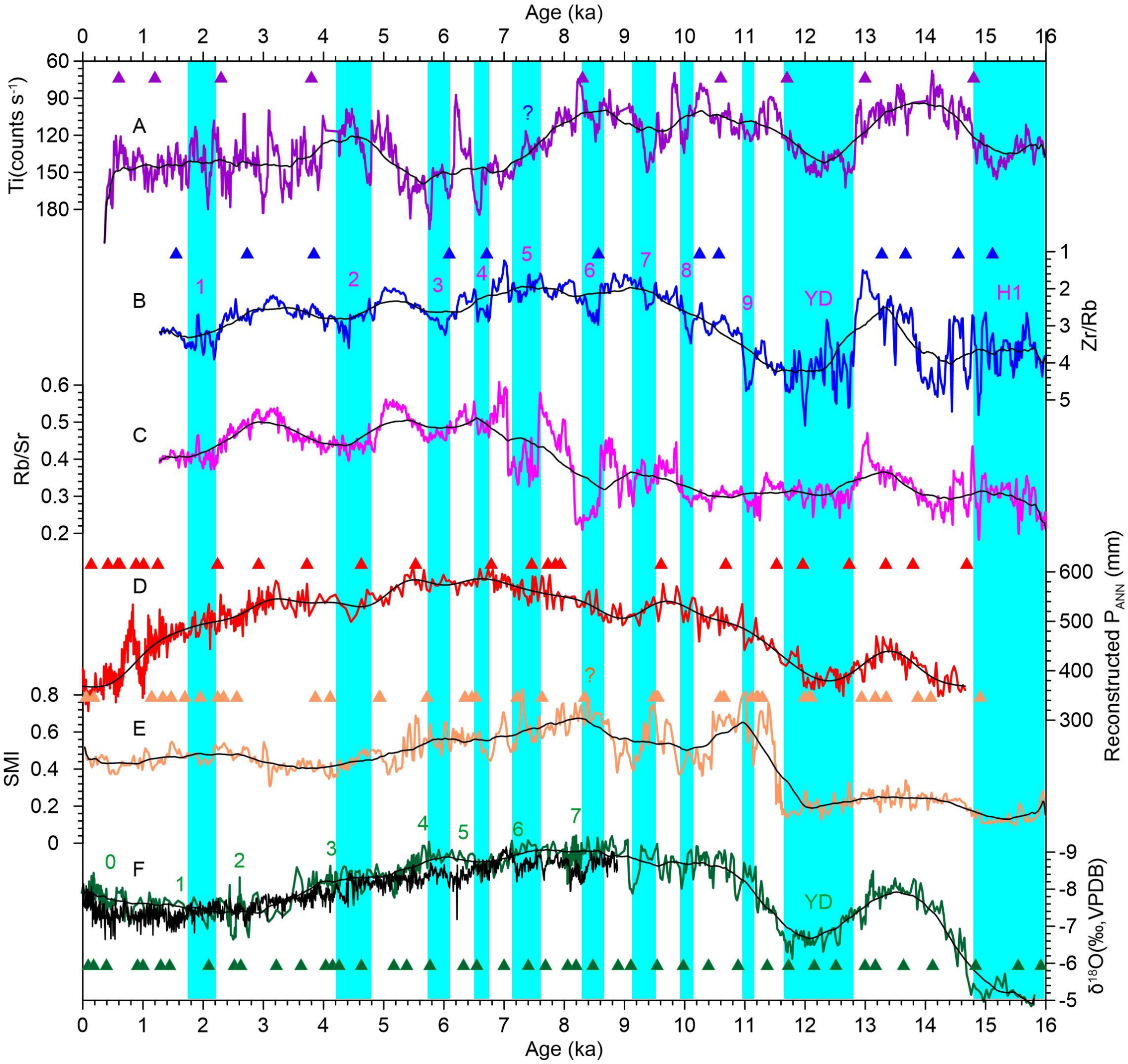

Fig 3. Comparisons of DDW records and other paleoclimatic records. (A) Ti content of Lake Huguang Maar (Yancheva et al., 2007); (B) Zr/Rb of DDW core; (C) Rb/Sr of DDW core; (D) Pollen-based annual precipitation (PANN) reconstructed from Gonghai Lake (Chen et al., 2015); (E) Lake Qinghai summer monsoon index (SMI) (An et al., 2012); (F) Speleothem $\delta^{18}O$ from Dongge Cave (Dykoski et al., 2005; Wang et al., 2005). AMS ^{14}C ages are marked on the records of Lake Huguang Maar (Purple triangle), DDW (Blue triangle), Gonghai Lake (Red triangle), and Lake Qinghai (Peach triangle), respectively. The ^{230}Th ages (Green triangle) are shown on

the speleothem records. The cyan bars indicate the timing of abrupt monsoon events in different records.

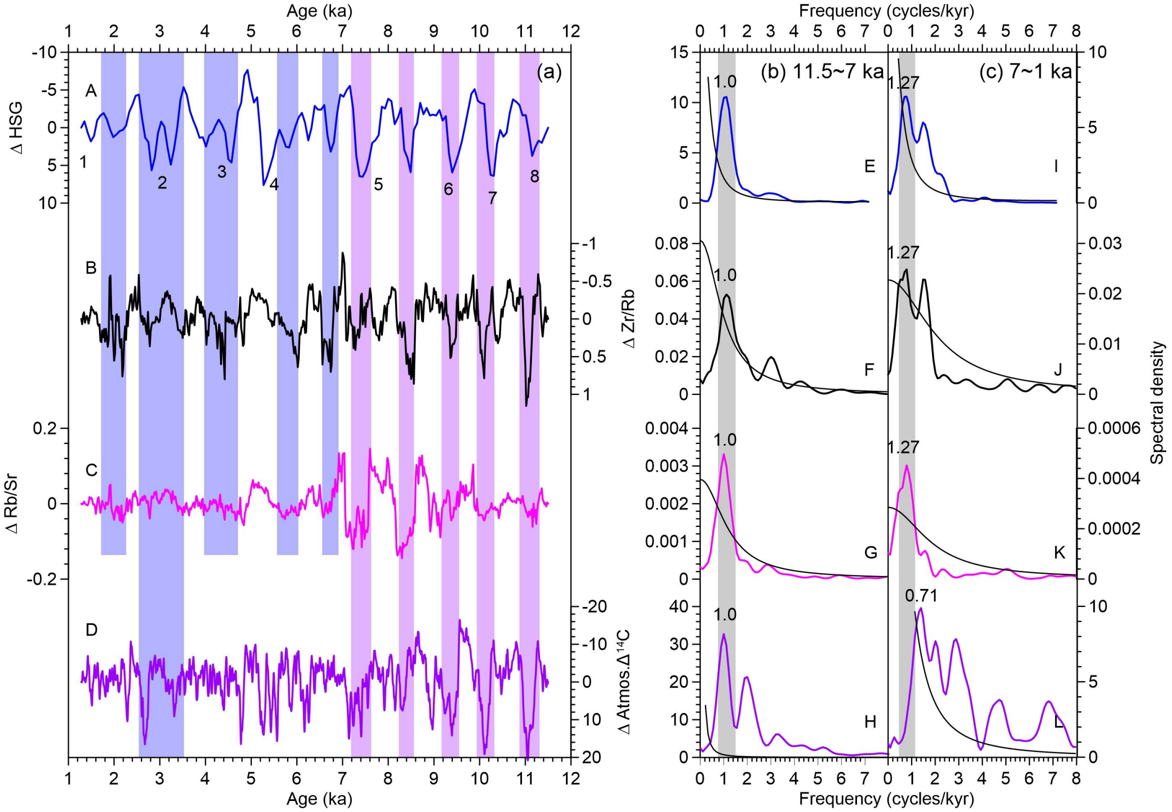

Fig 4. Centennial components (a) of Zr/Rb (B) and Rb/Sr (C) with the North Atlantic HSG (Bond et al., 2001) (A) and atmosphere △^{14}C record (Reimer et al., 2013) (D). The purple and blue bars indicate abrupt monsoon events. The right panel shows the spectra of the proxy records during the early (b) and late Holocene (c). Spectral peaks that are above the 80% confidence levels (black lines) are marked. The grey vertical bands indicate the most significant cycle.